

Modelling the heat dynamics of a building using stochastic differential equations

Klaus Kaae Andersen ^{a,*}, Henrik Madsen ^a, Lars H. Hansen ^b

^a Department for Mathematical Modelling, Technical University of Denmark, DK-2800 Lyngby, Denmark

^b VEA, Risø, DK-4000 Roskilde, Denmark

Received 9 October 1998; received in revised form 13 October 1998; accepted 13 October 1998

Abstract

This paper describes the continuous time modelling of the heat dynamics of a building. The considered building is a residential like test house divided into two test rooms with a water based central heating. Each test room is divided into thermal zones in order to describe both short and long term variations. Besides modelling the heat transfer between thermal zones, attention is put on modelling the heat input from radiators and solar radiation. The applied modelling procedure is based on collected building performance data and statistical methods. The statistical methods are used in parameter estimation and model validation, while physical knowledge is used in forming the model structure. The suggested lumped parameter model is thus based on thermodynamics and formulated as a system of stochastic differential equations. Due to the continuous time formulation the parameters of the model are directly physical interpretable. Finally, the prediction and simulation performance of the model is illustrated. © 2000 Elsevier Science S.A. All rights reserved.

Keywords: Stochastic differential equations; Heat dynamics; Parameter estimation; ML method

1. Introduction

The use of models for the heat dynamics in a building is a perceptive and practicable method to reduce the energy consumption and to improve the thermal comfort. A model can serve as a useful tool in, e.g., selecting insulation materials, analyzing control strategies or in the design of a suitable heating system. Along with the varieties of applications, two different modelling procedures may be used. The traditional approach is to use knowledge of the physical building characteristics and models of subprocesses and by those means achieve a deterministic model. An alternative method is to use building performance data and statistical methods.

Various deterministic approaches are described in the literature (see e.g., Ref. [1]) while the literature on statistical approaches is less. A statistical approach, the *grey box modelling method*, is applied by Ref. [2] in order to derive a total model for the heat dynamics of a building with a single test room. The proposed model is formulated as a system of stochastic differential equations and a maximum likelihood (ML) method is used for estimation of the parameters in the continuous-time model, based on discrete-time building performance data. As argued in Ref. [2] there are in particular two main differences between the grey box modelling approach and the traditional deterministic approach. Firstly, while the traditional approach uses knowledge about the physical characteristics only, the grey box model structure can be identified using both knowledge about the physical characteristics of the building and information from building performance data. Secondly, while the traditional approach is kept in a deterministic framework, the grey box approach is kept in a stochastic framework. Hereby statistical methods can be applied in identifying a suitable parameterization. This is often a very difficult task using the traditional approach.

In this paper, the grey box modelling method is applied. The attention is focused on modelling the heat dynamics of the indoor air temperature in a residential like building when excited by various heat inputs, such as solar radiation and heat

* Corresponding author

from radiators. The building considered is a low energy test building from where building performance data from a planned experiment is used. The modelling task is extended compared to the model presented in Ref. [2]. It consists of modelling the heat dynamics in various rooms of the test building, each differently affected by solar radiation. Furthermore, the power from the radiators is not known completely and has to be modelled as well. As in Ref. [2], the test house is not inhabited. The grey box modelling method, introduced in Section 2, is used since both information from the physics as well as information from the data can be used in determining a reasonable parameterization. The test building is described in Section 3 followed by a description of the building performance data in Section 4. Using this information, a total model is presented in Section 5. The model is formulated in continuous time, in terms of stochastic differential equations. The continuous-time formulation ensures that the parameters of the model are directly physical interpretable, while the stochastic framework permits a description of the accuracy of the model. Statistical methods are used to identify, estimate and validate the suggested model. The results are presented in Section 6, and finally, a conclusion with discussion is given.

2. The modelling approach

In this section the applied modelling approach is introduced. The modelling procedure may be described by a flowchart, sketched in Fig. 1. It consists of three stages: identification, estimation and validation. The loop continues until an adequate parameterization of the model is found. In the following each stage will be further discussed.

2.1. Identifying the model structure

The first step in the modelling procedure is to select a model structure. Both information from physics and information from measurements are used to identify a suitable model parameterization. The most important variables can be recognized, and insight of the most important dynamics can be achieved by examination of measurements from the system. To model the impact from the assumingly most important variables, well known thermodynamic relationships are used, and formulated in terms of a system of ordinary differential equations

$$d\mathbf{X}_t = f(\mathbf{X}_t, \mathbf{U}_t, \boldsymbol{\theta}, t)dt, \quad (1)$$

where $\mathbf{X}_t \in \mathbb{R}^{n_x}$ is a vector of system states and the vector $\mathbf{U}_t \in \mathbb{R}^{n_u}$ contains the known inputs. Finally, $\boldsymbol{\theta} \in \mathbb{R}^{n_p}$ is a vector of parameters. The lumped model Eq. (1) provides a deterministic description of the evolution in time of the states of the system. It is obvious that any description of the form Eq. (1) gives only an approximation of the evolution of the true system. In order to use Eq. (1) as the foundation for a description of the true variation of the states a stochastic term is included in Eq. (1) leading to the following system of stochastic differential equation

$$d\mathbf{X}_t = f(\mathbf{X}_t, \mathbf{U}_t, \boldsymbol{\theta}, t)dt + G(\boldsymbol{\theta}, t)dW_t, \quad (2)$$

where W_t is a standard Wiener process and $G(\boldsymbol{\theta}, t)$ is a function describing how the disturbance is entering the system. There are several reasons for introducing a noise term in Eq. (1), referring to Ref. [3]: (1) Modelling approximations. The system described by Eq. (1) might be an approximation to the true system. (2) Unrecognized and unmodelled inputs may affect the evolution of the states. (3) Measurements of the input are noise-corrupted. For a discussion on the application of stochastic differential equations in physics (see Ref. [4]).

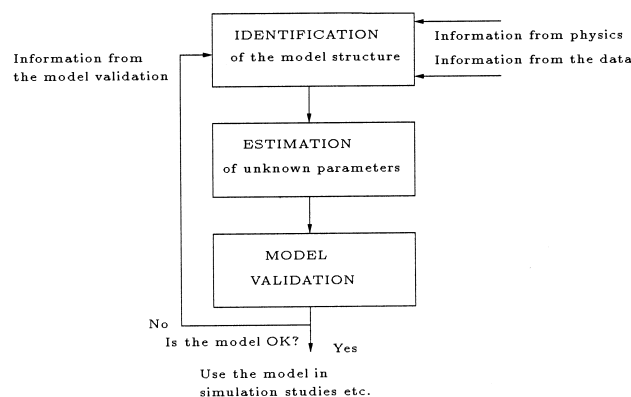


Fig. 1. The modelling procedure.

2.2. Applied estimation method

Having measured some function of the state variables, a state space representation can be formulated

$$d\mathbf{X}_t = f(\mathbf{X}_t, \mathbf{U}_t, \boldsymbol{\theta}, t)dt + G(\boldsymbol{\theta}, t)dW_t \quad (3)$$

$$\mathbf{Y}_t = h(\mathbf{X}_t, \mathbf{U}_t, \boldsymbol{\theta}, t) + \mathbf{e}_t \quad (4)$$

where \mathbf{Y}_t is a vector of the actually observed variables at the test building. Eq. (3) is a continuous-time system equation and Eq. (4) is the discrete time observation equation. The function h describes the relationship between the state variables \mathbf{X}_t and the measurements $\mathbf{Y}_t \in \mathbb{R}^{ny}$. $\mathbf{e}_t \in \mathbb{R}^{ny}$ is a vector describing the measurement noise which is assumed to be Gaussian distributed. The parameter vector $\boldsymbol{\theta}$ contains the equivalent thermal components, i.e., capacitances, resistances, and is estimated by a ML method. Descriptions of the ML method can be found in Refs. [5,6]. The software package Ref. [5], using the ML method, is used in estimating the parameter vector $\boldsymbol{\theta}$. Later on in the paper examples of a state space description will be illustrated.

2.3. Model validation

In the same manner as both building characteristics and information from data are used in identifying the model structure, the same information is used in validating the model. Since the model parameters are directly physical interpretable the behavior of the model should agree with the characteristics of the system, i.e., the estimated parameter vector $\hat{\boldsymbol{\theta}}$ should be close to the expected value. Simultaneously, the model should be able to predict the system with a reasonable accuracy. However, it is difficult to determine the goodness of fit using this criteria only. Therefore, various statistical tests are applied in validating the model, such as residual analysis, test for model order and parameter significance. In the modelling procedure information from the model validation is a useful tool in improving the model performance. If the model validation indicates an inadequate model performance, information from the model validation can indicate how to improve the model structure, as shown in Fig. 1, etc.

3. The test building

This section yields a description of the test building and its heating system. The purpose is to emphasize on the most important building characteristics and the influence from the heating system. This information is used in selecting a model structure for the heat dynamics in the test house. A more detailed description of the test building, the experimental design and the experiment can be found in Ref. [7].

The test building is located at the Technical University of Denmark (DTU), near Copenhagen, and was built around 1980. The term *low energy* refers to the nominal heat consumption, which is about 2.5 kW at -12°C outside and 20°C inside, i.e., a nominal heat loss of $\sim 78 \text{ W}/^\circ\text{C}$ [8]. The test building is a single-storeyed building with a non-ventilated crawl space and a roof space used as an office. The ground floor conforms a test area of 120 m^2 and is divided into three rooms, as sketched in Fig. 2. The test rooms, A_s and A_n , are used as test zones. The rooms are almost symmetrical and conforms each an area of 30 m^2 . Test room A_s has 3.6 m^2 window area facing south while test room A_n has 1.9 m^2 window area facing north. Room B is 60 m^2 and is used as a control zone. It contains some of the equipment for the experiment. All the windows in the control room are shield from solar radiation. The ceiling and the outer walls of the test building are light sandwich constructions based on a masonite beam insulated with 300 mm mineral wool, while the walls separating the rooms are insulated with 95 mm mineral wool. The floor in each room are layer constructions which makes the building thermal heavy and the use of insulation makes the building extremely tight. A water based central heating system is used for the heat supply. It consists of a heating unit, HU, placed in room B, and a radiator in each of the test

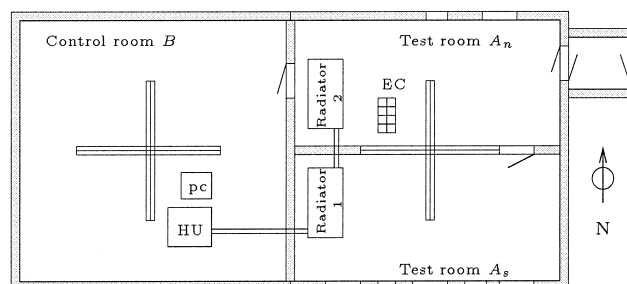


Fig. 2. A sketch of the test building and its interior.

rooms. The two radiators are identical with a nominal power of 395 W. The flow in each radiator is controlled by a thermostatic valve. An additional heat input is placed in room A_n , denoted EC. The EC-unit is remote controlled, a 0–5 V on/off signal controls an electrical on/off heat input of 0 or 150 W governed by a PRBS [9]. The idea of the EC is to compensate for the sparse solar radiation on the northern side of the test building [8]. Finally, the data acquisition system (PC) performs measurements of pressure, flow, temperature, light sensors, and consists of converter equipment and a computer, which is used to store the measured data obtained from experiments.

4. The data

In this section the dynamics of the most important variables will be discussed. The aim is to use this information in identifying the model structure. The experiment was carried out in the period 22 November–19 December 1996, and discussed in Ref. [7]. Measurements from this experiment are used in the modelling procedure. The following variables were measured at a frequency of 0.1 Hz:

T_i [°C]	indoor air temperature
T_u [°C]	outdoor air temperature
I [W/m ²]	solar radiation
T_s [°C]	supply temperature to radiator
T_r [°C]	return temperature from radiator
q [l/h]	flow in radiator

The air temperatures were measured at several points in each of the three rooms, while the outdoor temperature and the solar radiation were measured on the southern and northern side of the test building. Finally, the supply and return temperatures as well as the flow were measured at the radiator in each test room. Measurements of the air temperatures are plotted in Fig. 3. Considering these time series, the dynamics of the air temperatures in the three rooms are excited quite differently. This is as planned due to the experimental design, which has been performed to obtain the most informative data [7]. In order to excite the system, the experiment is started while the temperature in the building is low, i.e., the heating system has been shut down for a while in advance. The temperatures move towards a stationary temperature in the test rooms, due to the different heat inputs. The stationary temperature is determined by the set points of thermostatic valves, controlling the flow in the radiators. In the control room, B, the temperature T_b is increasing slowly. The main heat input to the control room is probably the heat loss from the heating unit and the conductive heat transfer from the test rooms. Since the test building is extremely tight, this explains the slow increment of the temperature. The solar radiation and the radiator flows, depicted in Figs. 4 and 5, respectively, affect the dynamics of the test room temperatures very differently. In the southern test room, A_s , the air temperature T_s is increasing rapidly when the solar radiation is high. Due to the thermostatic valve, the flow of water in the radiator q_s is reduced each time the solar radiation is high. Hence, the radiator flow and the solar radiation are strongly correlated. On the northern side of the test building the measured solar radiation I_n is severely

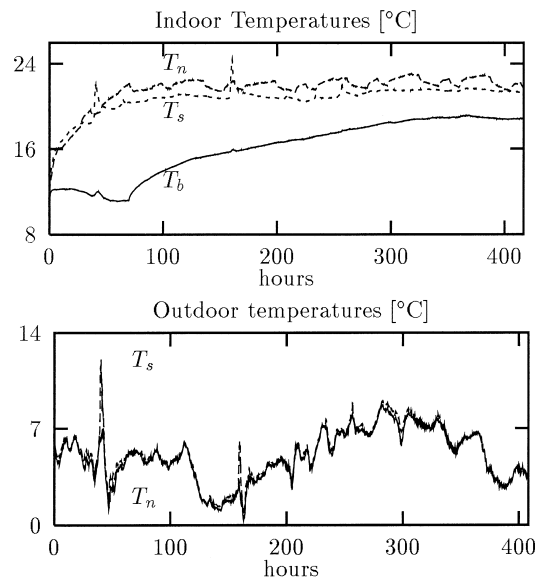


Fig. 3. Measured temperatures from an experiment at the test building. The indexes are as follows: s denotes south, n north and b the control room.

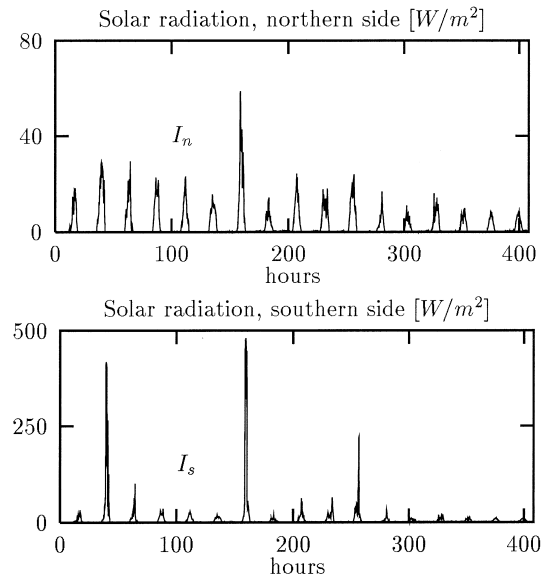


Fig. 4. Measurements of solar radiator.

limited compared to the radiation on the southern side of the test building. Only a part of the diffuse solar radiation is measured on the northern side. The power from the EC-unit (150 W) is the main heat input for the northern test room A_n , and only a very little flow, q_n , is required to maintain a stationary temperature. Thus, the main heat inputs and hereby the excitation of the test rooms temperatures are different. The main heat source in the northern test room is the EC-unit while the main heat source in the southern test room is the solar radiation and the power from the radiator.

5. Formulation of a model

In this section the formulation of a linear model for the variations of the test room air temperatures is proposed. The following items are considered important: (1) The model should be able to describe all the dynamics of interest in the room air temperatures, including the impact from the solar radiation and the radiator power. (2) The model should be formulated in continuous time in order to have parameters which are physical interpretable. (3) The model order should be as low as possible.

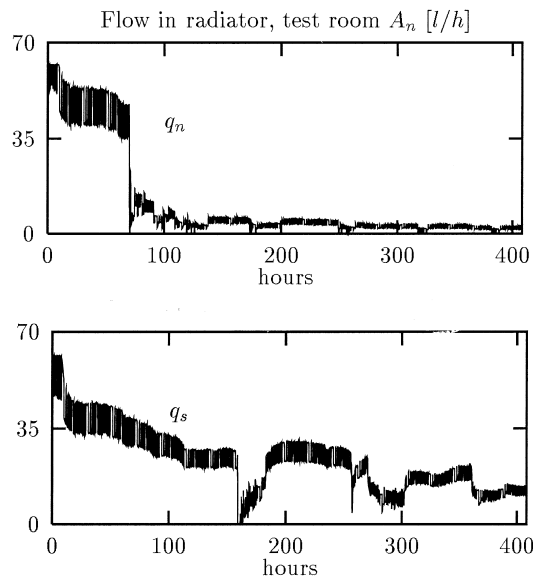


Fig. 5. Measurements of radiator flow.

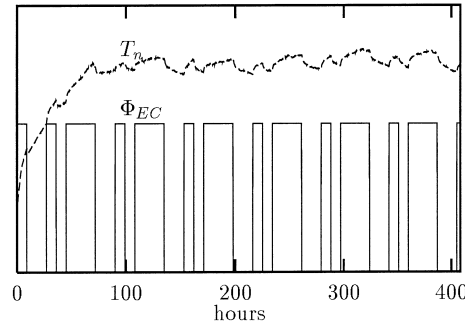


Fig. 6. The heat output from the EC-unit and the temperature in the northern test room.

Besides the information from the measurements in Figs. 3–5, additionally, information from the measurements is obtained. In Fig. 6 the output from the EC-unit and the temperature T_n in the northern test room, A_n , is shown. Considering the variations in the room air temperature, both a quick response after the input is shifted and a more persistent response are recognized. This indicates that at least two time constants are required for describing the short-term and the long-term variations of the room air temperatures in each test room, i.e., a second order model. In order to model both the short-term and the long-term variations, the heat dynamics of the room air and of the thermal heavy constructions are considered. This approach is described in Ref. [2] and it is found useful if the short-term variations of the room air temperature are important, as for instance when controllers containing a feedback from the room air temperature are considered. While the information from the data indicates that at least a second order model is required, the attention is turned towards the test building. The goal is to obtain some equations describing the heat dynamics of the room air and the thermal heavy constructions, which in this particular case is the floor. Hereby, each test room are regarded as two different thermal zones, the air and the floor. The heat equations for each zone are formed by considering the heat transfer, i.e., conduction, convection and radiation, that is assumed to have greatest influence on the heat dynamics in the test building. As argued in Section 4, it is assumed that the most important heat transfer that influences on the room air temperature are heat input from solar radiation, the EC-unit, the radiators and conductive heat transfer through the walls and floor in each room, as sketched in Fig. 7. Similarly, the most important heat transfer that directly affects the temperature of the floor are assumed to be heat input from solar radiation and conductive heat transfer from the room air. Taking the model approximations into account, neglecting further heat transfer, the heat dynamics can be expressed as a system of ordinary differential equations (see e.g., Ref. [10])

$$\frac{d(\text{Heat stored})}{dt} = \Sigma \text{Power in} - \Sigma \text{Power out} \quad (5)$$

$$\Rightarrow C_i \frac{dT_i}{dt} = \Sigma \Phi_{\text{in}} - \Sigma \Phi_{\text{out}}, \quad (6)$$

where C [J/(K °C)] denotes heat capacity, T denotes temperature (°C) and Φ (W) the heat transfer that is appraised to influence on the heat dynamics. To derive a parameterization for Φ , well known deterministic expressions for convective, conductive and radiate heat transfer are applied. The conductive heat transfer through the walls and floor are modelled by a simple first order differential equation

$$C \frac{dT}{dt} = \Phi_w = B_w (T_j - T_i), \quad (7)$$

where B_w (W/°C) is the thermal conductivity for a specific wall or floor w , and T_i (°C) and T_j are the temperatures at each side of the wall or floor. When using Eq. (7) it is assumed, that the heat transfer is one-dimensional. The assumed heat conduction is sketched in Fig. 8. The heat conduction between the air and the floor is sketched in Fig. 9. Note that only the

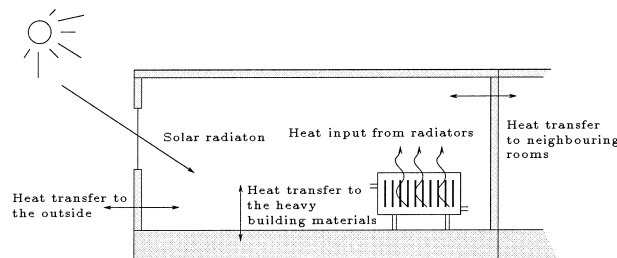


Fig. 7. A sketch of the heat transfer in the test house. The arrows symbolize the heat transfer that is assumed to be most important for the heat dynamics.

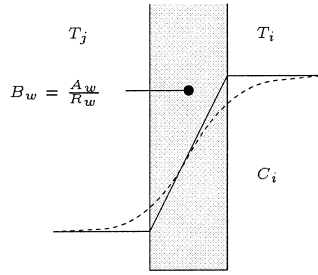


Fig. 8. Model approximations for the conductive heat transfer through a wall.

heat capacity of the floor and the air are modelled. Since the walls of the test building are light, it is assumed that the heat capacities of the walls can be neglected. Hence, the heat capacities of the walls are included in the ‘heat capacity of the air’, and only the thermal resistance of the walls are modelled.

To model the transmitted power from solar radiation, Φ_s (W), the following relationship is used

$$\Phi_s = IA_e, \tag{8}$$

where A_e (m^2) denotes an effective window area and I (W/m^2) is the measured solar radiation. In Eq. (8) it is expected that A_e for the considered building will be about 60% of the measured window size, since only a fraction of the solar radiation will be transmitted to the inside of the test building. The remaining part will be reflected and/or absorbed by the window [11]. Furthermore, it is assumed, that both the air temperature and the floor temperature are affected by the solar radiator, i.e., a fraction p of the solar radiation Φ_s is transmitted directly to the floor while the remaining part, $(1 - p)$, will directly heat the air. Hereby, the input from solar radiation is modelled as

$$\Phi_{s,air} = (1 - p)IA_e \quad \Phi_{s,floor} = pIA_e. \tag{9}$$

Now, Eq. (5) can be used to describe the heat dynamics for the temperature of the air and floor in a single test room, respectively,

$$C_i \frac{dT_i}{dt} = \sum_{walls} B_w(T_j - T_i) + B_a(T_a - T_i) + (1 - p)\Phi_s + \Phi_r + \Phi_{EC} \tag{10}$$

$$C_a \frac{dT_a}{dt} = B_a(T_i - T_a) + p\Phi_s \tag{11}$$

In Eq. (10) the power from the radiators is denoted Φ_r . The heat output from the EC-unit is known quite well, and is not modelled. In the following different models for Φ_r will be suggested. A simple model (see e.g., Ref. [12]) is given by

$$\Phi_r = c_p \rho q(T_f - T_r), \tag{12}$$

where c_p (W/K) is the specific heat capacity of the water in the radiator, ρ (kg/m^3) is the mass density of the water, q (m^3/s) is the flow and T_f and T_r ($^{\circ}C$) is the supply and return water temperature. Eq. (12) simply states that the power from the radiators is equal to the change in energy of the water, when it runs through the radiator. Another simple model is given by

$$\frac{dQ}{dt} = cT_d \quad \text{where } T_d = \frac{T_f + T_r}{2} - T_i, \tag{13}$$

where c is a constant. Eq. (13) is reported to be useful in situations where the flow is not too varying [13].

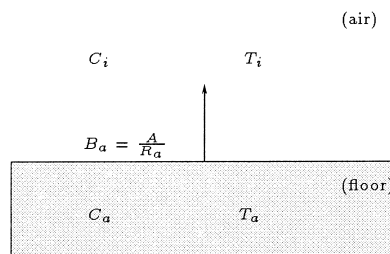


Fig. 9. The conductive heat transfer between the air and the floor.

If it is important to model the dynamics of the radiator as well, the following first order equation (see e.g., Ref. [14]) can be used

$$C_r \frac{dT_{\text{rad}}}{dt} = c_p \rho q (T_f - T_r) - B_r (T_{\text{rad}} - T_1)^n, \quad (14)$$

where T_{rad} is the mean temperature of radiator surface and n is the radiator exponent [7]. When using Eq. (12) or Eq. (13) to model the radiator power each test room is modelled by two differential equations, as in Eqs. (10) and (11). Using Eq. (14) implies three equations for each room. Thus, using the radiator model Eq. (12) or Eq. (13) a model for the heat dynamics of the test building can be formulated

$$C_{i,s} \frac{dT_{i,s}}{dt} = B_{u,s}(T_{u,s} - T_{i,s}) + B_b(T_b - T_{i,s}) + B_n(T_{i,n} - T_{i,s}) + B_{a,s}(T_{a,s} - T_{i,s}) + \Phi_{r,s} + A_{e,s}(1 - p_s)I_s \quad (15)$$

$$C_{a,s} \frac{dT_{a,s}}{dt} = B_{a,s}(T_{i,s} - T_{a,s}) + p_s A_{e,s}I_s \quad (16)$$

$$C_{i,n} \frac{dT_{i,n}}{dt} = B_{u,n}(T_{u,n} - T_{i,n}) + B_b(T_b - T_{i,n}) + B_n(T_{i,s} - T_{i,n}) + B_{a,n}(T_{a,n} - T_{i,n}) + \Phi_{r,n} + \Phi_{\text{EC}} + A_{e,n}(1 - p_n)I_n \quad (17)$$

$$C_{a,n} \frac{dT_{a,n}}{dt} = B_{a,n}(T_{i,n} - T_{a,n}) + p_n A_{e,n}I_n \quad (18)$$

The parameters in Eqs. (15)–(18) are specified in the nomenclature. The system of differential equations, Eqs. (15)–(18), is obvious an approximation to the true system. According to the discussion in Section 2, the system is formulated in terms of stochastic differential equations, yielding the linear state space description

$$d\mathbf{X} = \mathbf{A}\mathbf{X}dt + \mathbf{B}\mathbf{U}dt + d\mathbf{W}, \quad (19)$$

$$\mathbf{Y} = \mathbf{C}\mathbf{X} + \mathbf{D}\mathbf{U} + \mathbf{e}. \quad (20)$$

Eqs. (15)–(18) written matrix form, Eqs. (19) and (20), becomes

$$\begin{bmatrix} \frac{dT_{i,s}}{dt} \\ \frac{dT_{a,s}}{dt} \\ \frac{dT_{i,n}}{dt} \\ \frac{dT_{a,n}}{dt} \end{bmatrix} = \begin{bmatrix} \frac{-(B_{u,s} + B_b + B_n + B_{a,s})}{C_{i,s}} & \frac{B_{a,s}}{C_{i,s}} & \frac{B_n}{C_{i,s}} & 0 \\ \frac{B_{a,s}}{C_{a,s}} & \frac{-B_{a,s}}{C_{a,s}} & 0 & 0 \\ \frac{B_n}{C_{i,n}} & 0 & \frac{-(B_{u,n} + B_b + B_n + B_{a,n})}{C_{i,n}} & \frac{B_{a,n}}{C_{i,n}} \\ 0 & 0 & \frac{B_{a,n}}{C_{a,n}} & \frac{-B_{a,n}}{C_{a,n}} \end{bmatrix} \times \begin{bmatrix} T_{i,s} \\ T_{a,s} \\ T_{i,n} \\ T_{a,n} \end{bmatrix} + \begin{bmatrix} \frac{B_{u,s}}{C_{i,s}} & \frac{B_b}{C_{i,s}} & \frac{1}{C_{i,s}} & \frac{A_{e,s}(1-p_s)}{C_{i,s}} & 0 & 0 & 0 & 0 \\ 0 & 0 & 0 & \frac{p_s A_{e,s}}{C_{a,s}} & 0 & 0 & 0 & 0 \\ 0 & \frac{B_b}{C_{i,n}} & 0 & 0 & \frac{B_{u,n}}{C_{i,n}} & \frac{1}{C_{i,n}} & \frac{1}{C_{i,n}} & \frac{(1-p_n)A_{e,n}}{C_{i,n}} \\ 0 & 0 & 0 & 0 & 0 & 0 & 0 & \frac{p_n A_{e,n}}{C_{a,n}} \end{bmatrix} \times \begin{bmatrix} T_{u,s} \\ T_b \\ \Phi_{r,s} \\ I_s \\ T_{u,n} \\ \Phi_{r,n} \\ \Phi_{\text{EC}} \\ I_n \end{bmatrix} + \begin{bmatrix} dw_1 \\ dw_2 \\ dw_3 \\ dw_4 \end{bmatrix} \quad (21)$$

$$\begin{bmatrix} Y_1 \\ Y_2 \end{bmatrix} = \begin{bmatrix} 1 & 0 & 0 & 0 \\ 0 & 0 & 1 & 0 \end{bmatrix} \times \begin{bmatrix} T_{i,s} \\ T_{a,s} \\ T_{i,n} \\ T_{a,n} \end{bmatrix} + \begin{bmatrix} 0 & 0 & 0 & 0 & 0 & 0 & 0 & 0 \\ 0 & 0 & 0 & 0 & 0 & 0 & 0 & 0 \end{bmatrix} \times \begin{bmatrix} T_{u,s} \\ T_b \\ \Phi_{r,s} \\ I_s \\ T_{u,n} \\ \Phi_{r,n} \\ \Phi_{EC} \\ I_n \end{bmatrix} + \begin{bmatrix} e_1 \\ e_2 \end{bmatrix} \quad (22)$$

6. Results

In this section the model performance is presented. The model parameters are estimated using the ML method and building performance data. The applied data covers the period of 17 days from the test building as discussed in Section 4. Before estimating the parameters, the data has been subsampled to a sampling time of 10 min. This sampling time is chosen based on the a priori estimate of the smallest time constant, which is 20 min, along with Shannon's theorem.

By using the modelling procedure discussed in Section 2 it is found that the radiator power in the test rooms have to be modelled differently due to different excitation of the input variables. It is found that the diffuse solar radiation on the northern side of the test building does not influence the heat dynamics in the northern test room significantly. Contrary, the solar radiation on the southern side of the test building has a major impact on the heat dynamics in the southern test room. It is found that only the air temperature is directly affected by solar radiation, i.e., the estimate of the fraction p is zero. Due to the fact that the radiators in the test rooms are controlled by thermostatic valves, the radiator power and the solar radiation are strongly correlated. This implies that Eq. (13) is suitable in modelling the radiator power in the northern test room while Eqs. (12) and (14) are found adequate in the southern test room. The estimates and standard deviations of the remaining model parameters of the model are shown in Table 1.

It should be noted that only the thermal equivalent parameters of the model Eqs. (15)–(18), which are found significant, are tabulated. The parameters values seems reasonable compared to their expected values. However, the estimated values of the capacity of the indoor air are quite large. This can be explained by the fact, that not only the capacity of the air is modelled, but also the heat capacity of the interior in the test rooms and probably the inner part of the walls, as also reported in Ref. [3]. From that point of view, the estimates seem very reasonable and indicates in that the model parameterization is suitable. Furthermore, the estimates of the time constants, $\hat{\tau}_i$ are calculated by the eigenvalues, λ_i of the system matrix \mathbf{A} , i.e., $\hat{\tau}_i = -1/\lambda_i$. The estimated time constants, $\hat{\tau}_i$, are listed in Table 2. These estimates are close to their expected values. The heat dynamics of the air is fast compared to the slow heat dynamics of the floor, which was expected.

The model residuals have been analyzed to test if the residuals from the model can be accepted as being white noise. If this is the case, the model describes all the information given in the measurements. Test for white noise is applied through estimation of the cumulated periodogram Eq. (23) and the autocorrelation function Eq. (24)

$$\hat{C}(v_j) = \frac{\sum_{i=1}^j \hat{I}(v_i)}{\sum_{i=1}^{N/2} \hat{I}(v_i)} \quad (23)$$

Table 1
Parameter estimates of the model Eqs. (15)–(18)

Symbol	Estimate	Unit	Standard deviation
$B_{u,s}$	12.65	kJ/(K h)	0.60
B_b	32.39	kJ/(K h)	0.93
B_n	38.95	kJ/(K h)	0.91
$B_{a,s}$	542.18	kJ/(K h)	11.65
$B_{u,n}$	28.35	kJ/(K h)	0.25
$B_{a,n}$	624.34	kJ/(K h)	1.91
$C_{i,s}$	421.28	kJ/K	7.76
$C_{a,s}$	1531.85	kJ/K	67.46
$C_{i,n}$	810.19	kJ/K	15.75
$C_{a,n}$	3314.74	kJ/K	180.02
$A_{e,s}$	1.67	m ²	0.02

Table 2
Estimated time constants

	Northern room	Southern room	Unit
τ_{air}	25	42	min
τ_{floor}	23	26	h

where \hat{I} equals:

$$\hat{I}(v_i) = \frac{1}{N} \left(\sum_{t=1}^N \varepsilon(t) \cos(2\pi v_i t) \right)^2 + \frac{1}{N} \left(\sum_{t=1}^N \varepsilon(t) \sin(2\pi v_i t) \right)^2,$$

$$\hat{\rho}(k) = \frac{1}{N\hat{\sigma}_\varepsilon^2} \sum_{t=1}^{N-|k|} (\varepsilon(t) - \hat{\varepsilon}_\mu)(\varepsilon(t+|k|) - \hat{\varepsilon}_\mu), \quad (24)$$

where ε_t denotes the prediction error or residual at time t . Hence, the residuals are analyzed in both the frequency and time domain. The predicted states and the equivalent measurements cannot be distinguished in a graph, and is therefore not plotted. However, the statistical tests, Eqs. (23) and (24) may be shown visually. In Fig. 10 the residuals from each test room are compared with the approximated 95% interval of significance. The statistical tests show, that the residuals of each test room can be regarded as white noise. This implies that the model order is sufficient. Finally, a simulation performance of the model using the estimated parameters is shown in Fig. 11. Considering that the temperatures were measured with an accuracy of 0.25°C and that the maximum difference between the simulated and measured temperatures, i.e., the simulation error, is 0.40°C during the period of 17 days, the simulation performance is considered excellent.

7. Conclusion

In this paper a lumped parameter model describing the heat dynamics of a residential like building has been proposed. The selected modelling method was the grey box modelling approach, i.e., the model was kept in a stochastic framework and the model structure was identified using both information from building performance data as well as known thermal properties. The model was formulated as a system of stochastic differential equations and statistic methods were applied for identifying, estimating and validating the model.

The heat dynamics in two test rooms were modelled. The two test rooms were facing opposite directions, north and south, respectively, and were hereby very differently affected by the solar radiation. Each test room was divided into two thermal zones in order to model both the short term and the long term variations. Furthermore, submodels for the radiator power and the solar radiation were presented. Finally, a linear state space model was formulated, in terms of stochastic differential equations.

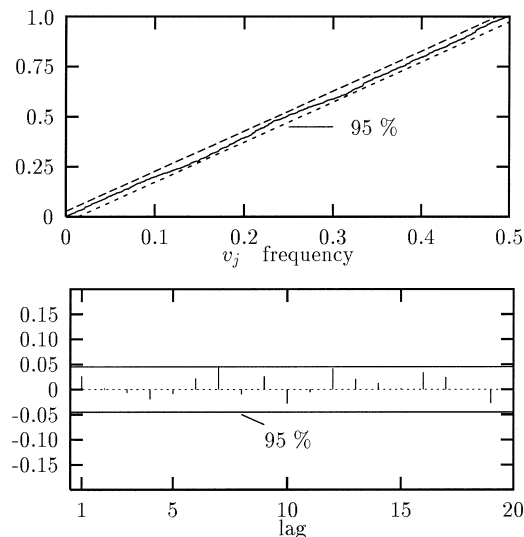


Fig. 10. Residual analysis of the prediction error. Top: cumulated periodogram for the residuals of the southern air temperature. Bottom: autocorrelation function for the residuals of the northern air temperature. In both cases, the residuals can be assumed to be white noise.

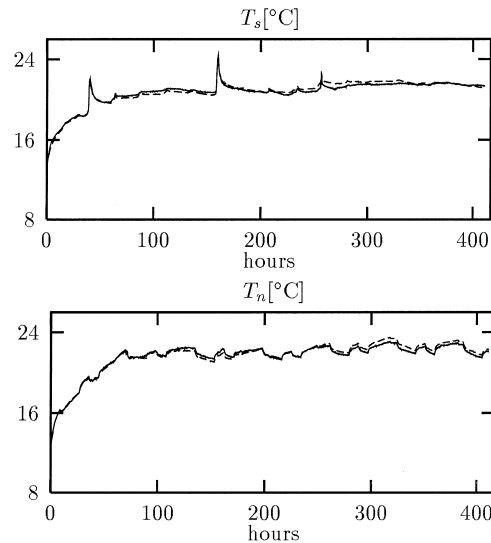


Fig. 11. Simulation performance during 17 days. Top: simulation performance of the air temperature in the southern test room. Bottom: simulation performance of the air temperature in the northern test room.

The model parameters were estimated using a ML method. Through statistical tests and physical interpretation of the system, it was argued, that the model gives a good description of the heat dynamics of the considered building. Different models for the radiator power were found suitable in each test room due to the very different influence from the solar radiation on the northern and southern side of the building, respectively. Furthermore the radiator power, which was controlled by thermostatic valves, were strongly correlated with the solar radiation and affected the choice of radiator models. The estimated parameters seemed reasonable compared to the expected values of the equivalent thermal components. Furthermore, the residuals from the model could be accepted as being white noise, which indicated that the model describes all the variation in the data. Finally, it was shown that the model was able to simulate the system with a very high accuracy.

8. Nomenclature

	Symbol		Unit
Model states	$T_{i,s}$	Air temperature, room A_s	°C
	$T_{a,s}$	Floor temperature, room A_s	°C
	$T_{i,n}$	Air temperature, room A_n	°C
	$T_{a,n}$	Floor temperature, room A_n	°C
Model inputs	T_b	Air temperature, room B	°C
	$T_{u,s}$	Outside air temperature on the southern side	°C
	$T_{u,n}$	Outside air temperature on the northern side	°C
	I_s	Solar radiation at the southern side	W/m ²
	I_n	Solar radiation at the northern side	W/m ²
	$\Phi_{r,s}$	Power from radiator, room A_s	W
	$\Phi_{r,n}$	Power from radiator, room A_n	W
	Φ_{EC}	Power from EC-unit, room A_n	W
Model parameters	$A_{e,s}$	Effective window area facing south	m ²
	$A_{e,n}$	Effective window area facing north	m ²
	$B_{u,s}$	Conductivity coefficient from room A_s to the outside	kJ/(K h)
	$B_{u,n}$	Conductivity coefficient from room A_n to the outside	kJ/(K h)
	B_b	Conductivity coefficient from room A_s and A_n to room B	kJ/(K h)
	B_n	Conductivity coefficient from room A_s to A_n	kJ/(K h)
	$B_{a,s}$	Conductivity coefficient from the air to the floor, room A_s	kJ/(K h)

	$B_{a,n}$	Conductivity coefficient from the air to the floor, room A_n	$\text{kJ}/(\text{K h})$
	$C_{i,s}$	Heat capacity of the air, room A_s	kJ/K
	$C_{a,s}$	Heat capacity of the floor, room A_s	MJ/K
	$C_{i,n}$	Heat capacity of the air, room A_n	kJ/K
	$C_{a,n}$	Heat capacity of the floor, room A_n	MJ/K
	p_s	Fraction of solar radiation transmitted to the floor, room A_s	–
	p_n	Fraction of solar radiation transmitted to the floor, room A_n	–
	$e_{(\cdot)}$	Measurement error	$^{\circ}\text{C}$
	$dw_{(\cdot)}$	System error	$^{\circ}\text{C}$
Model outputs	Y_1	Air temperature, room A_s	$^{\circ}\text{C}$
	Y_2	Air temperature, room A_n	$^{\circ}\text{C}$

References

- [1] J.W. Mitchell, W.A. Beckman (Eds.), Building Simulation '95, Fourth International Conference Proceedings, Madison, WI, USA, August 1995, International Building Performance Simulation Association.
- [2] H. Madsen, J. Holst, Estimation of continuous-time models for the heat dynamics of a building, *Energy and Buildings* 22 (1995) 67–79.
- [3] H. Madsen, J. Holst. Modelling non-linear and non-stationary time series (lecture notes), Jan. 1996.
- [4] B. Øksendal, Stochastic Differential Equations, Springer-Verlag, 1985.
- [5] H. Madsen, H. Melgaard, CTLSM—version 2.6 (program manual), IMM, DTU, 1993.
- [6] J.N. Nielsen, H. Madsen, H. Meelgaard, M. Baadsgaard, Estimation of embedded parameters in stochastic differential equations using discrete-time measurements, 1998, to be published.
- [7] L.H. Hansen, Stochastic modelling of central heating systems, PhD thesis, IMM, DTU, 1997.
- [8] L.H. Hansen, Dynamic analysis of a low energy test house and a central heating system, Technical Report 20, IMM, DTU, 1996.
- [9] K.R. Godfrey, Correlation methods, *Automatica* 16 (1980) 527–534.
- [10] L. Ljung, T. Glad, Modelling and Simulation (in Swedish), Studentlitteratur, Lund, 1991.
- [11] Hansen, Kjerulf-Jensen, Stampe (Eds.), Heating and Thermal Comfort (in Danish), DANVAK ApS, 1990.
- [12] O. Albrechtsen, Water Based Central Heating Systems (in Danish), 1992.
- [13] A. Benonysson, Dynamic Modelling and Operational Optimization of District Heating Systems, DTU, 1991.
- [14] K.K. Andersen, Stochastic modelling of energy systems (in Danish), Master's thesis, IMM, DTU, 1997.